Evidence of Ni(III) Disproportionation in the $TlNiO_3$ Perovskite Lattice through Neutron Powder Diffraction and Mössbauer Spectroscopy

S. J. Kim,[†] M. J. Martinez-Lope,[‡] M. T. Fernandez-Diaz,[§] J. A. Alonso,[‡] I. Presniakov,[||] and G. Demazeau*,[†]

Institut de Chimie de la Matière Condensée de Bordeaux (ICMCB-UPR.CNRS 9048), 87 avenue du Dr. A. Schweitzer, 33608 Pessac Cedex, France, and Ecole Nationale Supérieure de Chimie et de Physique de Bordeaux (ENSCPB), Laboratoire de Physico-Chimie des Hautes Pressions (Interface ENSCPB/ICMCB), 16 avenue Pey-Berland, 33607 Pessac Cedex, France, Instituto de Ciencia de Materiales de Madrid, C.S.I.C., Cantoblanco, E-28049 Madrid, Spain, Institut Laue-Lagevin, BP 156, 38042 Grenoble Cedex 9, France, and Chair of Radiochemistry, Mössbauer Group, Department of Chemistry, Lomonosov University, 119899 Moscow-V-234, Russia

Received March 7, 2002. Revised Manuscript Received September 23, 2002

$TlNiO_3$ has been prepared under high oxygen pressure. This perovskite has been characterized by high-resolution neutron powder diffraction (NPD), Mössbauer spectroscopy, and magnetic measurements. The crystal structure was refined in the monoclinic $P2_1/n$ space group, containing two crystallographic sites for Ni^{3+}, in such a way that expanded and contracted NiO_6 octahedra alternate along the three crystallographic directions. In this model the agreement factors are significantly better than those obtained after the refinement of the structure in the conventional space group *Pbnm* (orthorhombic symmetry). $TlNiO_3$ becomes antiferromagnetically ordered below $T_N = 104$ K. The low-temperature (2 K) magnetic structure, also studied from NPD data and characterized by a propagation vector $\mathbf{k} = (1/2, 0, 1/2)$, is similar to that observed for $YNiO_3$, and it is compatible with this two-sites model. A Mössbauer study of $TlNi_{0.98}{}^{57}Fe_{0.02}O_3$ confirms the existence of two octahedral sites for $^{57}Fe^{3+}$. All these results are in agreement with a Ni^{3+} disproportionation ($2Ni^{3+} \rightarrow Ni^{(3+\alpha)} + Ni^{(3-\alpha)+}$) phenomenon, already suggested for other $ANiO_3$ (A = rare earths or Y) perovskites through neutron diffraction data.

Introduction

The $ANiO_3$ perovskites (A = rare earth and Y) have been prepared for the first time in 1971 by using high oxygen pressures through the "in situ" thermal decomposition of $KClO_3$ in belt-type equipment.[1,2] An antiferromagnetic ordering was detected through magnetic measurements of the $ANiO_3$ perovskites with diamagnetic A^{3+} cations (A = Lu, Y).[2] When the structural distortion is increased—with the A^{3+} cations shrinking (from La to Lu)—the electronic localization is improved: if $LaNiO_3$ is a metal, $LuNiO_3$ is an insulator at room temperature.[3] Then a metal−insulator (MI) transition versus temperature was found to take place for the different A^{3+} cations (A = rare earth), at increasing temperatures as the ionic radius of A^{3+} decreases.[4,5]

Recently, a careful analysis of synchrotron X-ray and neutron diffraction data allowed the detection of two different sites for trivalent nickel in the crystal structure of $ANiO_3$, for the smaller rare-earth cations (A = Ho → Lu and Y) at room temperature. The splitting of the Ni sites accounts for the reduction in symmetry from orthorhombic to monoclinic (space group $P2_1/n$).[6−9] In this crystal structure, expanded and contracted $Ni1O_6$ and $Ni2O_6$ octahedra alternate along the three crystallographic directions. This behavior was interpreted as a charge disproportionation of Ni^{3+} cations, according to the equation $2Ni^{3+} \rightarrow Ni^{(3+\alpha)+} + Ni^{(3-\alpha)+}$. In fact, the charge disproportionation effect is only observed in the insulating charge-localized regime, below the MI transition that these perovskites experience as a function of

* To whom correspondences should be addressed. E-mail: demazeau@icmcb.u-bordeaux.fr. Tel: 33-(0)5-56-84-83-58. Fax: 33-(0)5-56-84-27-10.

[†] Institut de Chimie de la Matière Condensée de Bordeaux and Ecole Nationale Supérieure de Chimie et de Physique de Bordeaux.

[‡] Instituto de Ciencia de Materiales de Madrid.

[§] Institut Laue-Lagevin.

[||] Lomonosov University.

(1) Demazeau, G.; Marbeuf, A.; Pouchard, M.; Hagenmuller, P. *J. Solid State Chem*. **1971**, *3*, 582.

(2) Demazeau, G.; Pouchard, M.; Hagenmuller, P. *High Temp.-High Pressures* **1976**, *8*, 624.

(3) Demazeau, G. Thesis doctorat ès-Sciences Physiques, University Bordeaux 1, 1973, no. 419.

(4) Lacorre, P.; Torrance, J. B.; Pannetier, J.; Nazzal, A. I.; Wang, P. W.; Awang, T. C.; Siemens, R. L. *J. Solid State Chem*. **1991**, *91*, 225.

(5) Torrance, J. B.; Lacorre, P.; Nazzal, A. I.; Ansaldo, E. J.; Niedermayer, Ch. *Phys. Rev. B* **1992**, *45*, 8209.

(6) Alonso, J. A.; Martinez-Lope, M. J.; Casais, M. T.; Aranda, M. G.; Fernandez-Diaz, M. T. *J. Am. Chem. Soc.* **1999**, *121*, 4754.

(7) Alonso, J. A.; Garcia-Munoz, J. L; Fernandez-Diaz, M. T.; Aranda, M. A. G.; Martínez-Lope, M. J.; Casais, M. T. *Phys. Rev. Lett.* **1999**, *82*, 3871.

(8) Alonso, J. A.; Martínez-Lope, M. J.; Casais, M. T.; Garcia-Munoz, J. L.; Fernandez-Diaz, M. T. *Phys. Rev. B* **2000**, *61*, 1756.

(9) Alonso, J. A.; Martínez-Lope, M. J.; Casais, M. T.; Garcia-Munoz, J. L.; Fernandez-Diaz, M. T.; Aranda, M. G. *Phys. Rev. B* **2001**, *64*, 94102.

10.1021/cm021157o CCC: $22.00
Published on Web 11/26/2002

temperature. Above T_{MI} (in the 570−600 K range for A = Ho → Lu and Y) the electronic delocalization is concomitant with the adoption of the conventional orthorhombic *Pbnm* structure, with a single site for Ni^{3+}.[7,8]

All these studies involved $ANiO_3$ perovskites with rare earth as the A^{3+} cation, with the same electronic configuration $[(Xe)4f^n5d^06s^0$ $(0 < n < 14)]$. Therefore, the physical-chemical properties of these Ni^{3+} perovskites were correlated to the structural lattice distortion generally evaluated by the Ni−O−Ni angle. The objective of our work was to check the role of a (A^{3+}−O) bond with a different chemical nature ($A^{3+} \neq$ rare earth) both (i) on the structural distortion of the perovskite lattice and (ii) on the strength of the competing (Ni^{3+}−O) bonds. Consequently, due to size and electronic considerations, Tl^{3+} appeared as a good candidate, its size being between that of Yb^{3+} and Lu^{3+} and its electronic configuration $[(Xe)4f^{14}5d^{10}6s^0]$ being different from those of the rare-earth cations. In addition, the smallest difference of electronegativity between the Tl and O atoms compared to that between A and O (A = rare earth) would improve the covalence of the Tl^{3+}−O bond.

Previous structural studies using X-ray diffraction[10] have underlined that the presence of Tl^{3+} induces a different oxygen environment in the perovskite structure (4 + 4 + 4 Tl−O distances) compared to that conventionally observed for a $GdFeO_3$-type distortion (8 + 4 A−O distances). This is surprising since the A^{3+} size (A = rare earth) is comparable to that of Tl^{3+} and is an effect of the different electronic configuration of Tl^{3+}, of its higher electronegativity, and of its ability to form stronger, more covalent, chemical bonds to oxygen. In addition, the T_N value observed for $TlNiO_3$ is weaker than that expected on the basis of the Ni−O−Ni angle.[10,11] Consequently, a neutron diffraction analysis was considered to be important to evaluate the most suitable space group, *Pbnm* (1 Ni site) or $P2_1/n$ (2 Ni sites), to define the crystal structure and to investigate the possible presence of a charge disproportionation phenomenon, similar to that recently suggested for the smallest rare-earth cations, as well as to study the low-temperature magnetic structure of $TlNiO_3$.

Experimental

Synthesis of $TlNiO_3$. The preparation of $TlNiO_3$ implied two difficulties: (i) the thermal stabilization of Tl_2O_3 as a precursor and (ii) the oxidation of Ni^{2+} to Ni^{3+}. Consequently, high oxygen pressures have been developed using the thermal decomposition of $KClO_3$ as an oxygen source in the reaction cell of a belt-type apparatus. To improve the reactivity and shorten the reaction time, $Ni(OH)_2$ was used instead of NiO. The precursors Tl_2O_3, $Ni(OH)_2$, and $KClO_3$ were intimately mixed in the molar proportions 1:2:1 The optimized preparation conditions leading to a unique phase, mixed with KCl as a resulting product from the thermal $KClO_3$ decomposition, were $P = 7.5$ GPa, $T = 650$−700 °C, and $t = 2$−3 min. After reaction, KCl is readily leached out with distillated water. The nickel oxidation state (n+) was evaluated using chemical iodine titration and thermogravimetric analysis; in both cases the n+ value was close to 3+ $(2.96 < n < 2.98)$.[10]

(10) Kim, S. J.; Demazeau, G.; Alonso, J. A.; Choy, J. H. *J. Mater. Chem.* **2001**, *11*, 487.

(11) Kim, S. J.; Demazeau, G.; Presniakov, I.; Pokholok, K.; Sobolev, A.; Ovanesyan, N. *J. Am. Chem. Soc.* **2001**, *123*, 8127.

Table 1. Unit Cell Parameters, Atomic Positions, and Reliability Factors for $TlNiO_3$ at Room Temperature, Refined in the *Pbnm* Space Group

space group (*Pbnm*):
$a = 5.2544(1)$ Å, $b = 5.3674(2)$ Å, $c = 7.5609(2)$ Å, $V = 213.24$ Å^3, $Z = 4$, $R_{wp} = 4.53\%$, $R_{exp} = 3.06\%$, $R_{Bragg} = 6.02\%$, $\chi^2 = 2.16$

	site	G	x	y	z	B (Å^2)
Tl	4c	1	0.9868(4)	0.0595(3)	0.25	0.62(6)
Ni	4b	1	0.5	0	0	0.45(2)
O1	4c	1	0.1055(5)	0.4523(5)	0.25	0.76(4)
O2	8d	1	0.6981(4)	0.2989(2)	0.0568(2)	0.86(3)

Synthesis of $TlNi_{0.98}{}^{57}Fe_{0.02}O_3$. ^{57}Fe was used as a Mössbauer probe in a low concentration (2%) to minimize the possible perturbations in the $TlNiO_3$ lattice. The precursors used were Tl_2O_3 and $Ni_{0.98}{}^{57}Fe_{0.02}O$. The last one has been prepared in three steps: (i) the dissolution of an appropriate quantity of nickel nitrate $[Ni(NO_3)_2, 6H_2O]$ and ^{57}Fe (as metal) in a nitric acid solution (1 M), (ii) the precipitation of a mixed hydroxide using a KOH solution (3 M), and (ii) a thermal treatment of the resulting hydroxide issued from step (ii) at 300 °C.

The precursors Tl_2O_3 and $Ni_{0.98}{}^{57}Fe_{0.02}O$ were mixed with $KClO_3$—used as an oxygen source—in the molar proportion 1/2/1 and then put in a gold capsule inserted in the reaction cell of belt-type equipment. The experimental conditions were the same as those used for the $TlNiO_3$ synthesis (7.5 GPa, 650−700 °C, 2−3 min).

Magnetic and Mössbauer Measurements. The susceptibility and magnetization measurements were performed in a commercial SQUID magnetometer. The dc susceptibility was measured for temperatures ranging from 1.8 to 300 K. Isothermal magnetization curves were obtained at different temperatures in a magnetic field ranging from −50 to 50 kOe.

The ^{57}Fe Mössbauer spectra were recorded at 300 and 4.2 K using a conventional constant acceleration Mössbauer spectrometer. The radiation source $^{57}Co(Rh)$ was kept at room temperature. All isomer shifts refer to the α-Fe absorber at 300 K.

Neutron Powder Diffraction. A high-resolution neutron powder diffraction (NPD) pattern was acquired at room temperature with the D2B diffractometer of the Institut Laue-Langevin in Grenoble (France), with a wavelength of 1.594 Å. Despite the difficulties of such an experiment, given the relatively small amount of available sample (less than 0.8 g due to the high-pressure process required for the synthesis), a pattern with good statistics could be collected in the high-flux mode with a counting time of 8 h. A low-temperature (2 K) NPD pattern was also found with the high-flux multidetector D1B diffractometer, with a wavelength $\lambda = 2.525$ Å and a counting time of 30 min. This NPD pattern was used to determine the magnetic structure of $TlNiO_3$. The neutron diffraction data were analyzed by using the Rietveld method, and the refinements of the crystallographic and the magnetic structures were performed with the FULLPROF program. In the refinements, a pseudo-Voigt function was taken to simulate the profile and the background was fitted with a fifth-degree polynomial function. The scattering lengths of Tl, Ni, and O were 8.776, 10.300, and 5.803 fm, respectively.

Results and Discussion

Structural Analysis. The room-temperature NPD data were, at first, refined in the conventional orthorhombic *Pbnm* group. The final parameters are included in Table 1; the main interatomic distances and angles are listed in Table 2. This model considers a single site for Ni cations; the (NiO_6) octahedra exhibit average ⟨Ni−O⟩ distances close to 1.971(2) Å.

Due to fact that the Tl^{3+} ionic size is between those of Yb^{3+} and Lu^{3+} and considering a model recently described for the $ANiO_3$ perovskites with smaller rare

Table 2. Interatomic Distances and Bond Angles for $TlNiO_3$ Refined in the *Pbnm* Space Group

	multiplicity	distance (Å)		angle (deg)
Tl−O1	1	2.204(4)	O1−Ni−O2	86.9(1)
Tl−O1	1	2.251(3)	O1−Ni−O2	87.4(1)
Tl−O1	1	3.156(4)	O2−Ni−O2	86.9(1)
Tl−O1	1	3.264(3)		
Tl−O2	2	2.209(2)		
Tl−O2	2	2.496(2)	Ni−O1−Ni	144.2(4)
Tl−O2	2	2.698(2)	Ni−O2−Ni	146.1(8)
Tl−O2	2	3.408(2)	⟨Ni−O2−Ni⟩	145.5
Ni−O1	2	1.986(7)		
Ni−O2	2	1.960(2)	1.960(2)	1.960(2)
Ni−O2	2	1.966(2)	1.966(2)	1.966(2)
⟨Ni−O⟩		1.971	1.971	1.971

Table 3. Unit Cell Parameters, Atomic Positions, and Reliability Factors for $TlNiO_3$ at Room Temperature, Refined in the $P2_1/n$ Space Group

space group ($P2_1/n$):
$a = 5.2545(1)$ Å, $b = 5.3674(2)$ Å, $c = 7.5607(2)$ Å,
$\beta = 90.002(7)°$, $V = 213.23$ Å^3, $Z = 4$, $R_{wp} = 4.17\%$,
$R_{exp} = 3.08\%$, $R_{Bragg} = 4.86\%$, $\chi^2 = 1.82$.

	site	G	x	y	z	B (Å^2)
Tl	4e	1	0.9865(4)	0.04902(2)	0.2497(10)	0.62(3)
Ni1	2d	1	0.5	0	0	0.46(2)
Ni2	2c	1	0.5	0	0.5	0.46(2)
O1	4e	1	0.1061(5)	0.4527(5)	0.2406(10)	0.63(2)
O2	4e	1	0.691(1)	0.3088(8)	0.0520(8)	0.63(2)
O3	4e	1	0.206(1)	0.2154(8)	0.9396(8)	0.63(2)

earths (in the insulating regime, below T_{MI}), in which a reduction of symmetry from orthorhombic to monoclinic accounts for the existence of two independent (NiO_6) octahedra, a structure refinement of the NPD data was then performed in the monoclinic $P2_1/n$ space group, with unit-cell parameters related to a_0 (ideal cubic perovskite, $a_0 \approx 3.8$ Å) as $a \approx \sqrt{2}a_0$, $b \approx \sqrt{2}b_0$, $c \approx 2a_0$) using as the starting model the already reported structure for $YNiO_3$.[8] In $P2_1/n$, it is necessary to define two crystallographically independent Ni positions (Ni1 and Ni2) as well as three kinds of nonequivalent oxygen atoms (O1, O2, and O3) all in general (x, y, z) positions. The final atomic coordinates, unit-cell parameters, and discrepancy factors after the refinement are given in Table 3. Figure 1 shows the agreement between observed and calculated NPD profiles. Table 4 contains selected bond distances and angles. ($Ni1O_6$) and ($Ni2O_6$) octahedra are fully ordered and alternate along the three directions of the crystal, in such a way that each ($Ni1O_6$) octahedra is linked to six ($Ni2O_6$) octahedra, and vice versa. The monoclinic β angle is virtually equal to 90°: the metric of this monoclinic structure seems to be strongly pseudo-orthorhombic. The stability and consistency of the refinement (fast and unique convergence, reasonable standard deviations, and positive thermal factors) warrants the reliability of the refinement and seems to confirm the monoclinic internal symmetry of the $TlNiO_3$ sample, despite the exhibited pseudo-orthorhombic metric. The crystal structure consists, therefore, of a 1:1 ordered arrangement of expanded ($Ni1O_6$) and contracted ($Ni2O_6$) octahedra. At 300 K the difference in size between the large ($Ni1O_6$) octahedra

(⟨Ni1−O⟩ = 2.032(7) Å) and small ($Ni2O_6$) octahedra (⟨Ni2−O⟩ = 1.907(7) Å) is similar to that observed in $YNiO_3$. This result shows evidence for the stabilization of an uncompleted charge disproportionation, $2Ni^{3+} \rightarrow Ni^{(3+\alpha)+} + Ni^{(3-\alpha)+}$, very similar to that found in $ANiO_3$ for the smaller rare-earth cations (A = Y, Ho → Lu). It suggests also for $TlNiO_3$ the same charge disproportionation phenomenon. It seems that the stabilization of a charge density wave could be a universal feature of the whole family of nickelate(III) perovskites.

Magnetic Structure of $TlNiO_3$. A NPD pattern collected at 1.5 K with a D1B multidetector diffractometer with a wavelength $\lambda = 2.525$ Å was used to resolve the magnetic structure. The simultaneous refinement of the crystallographic and the magnetic structures were performed by using the Rietveld method with the FULLPROF program. In the 1.5 K NPD pattern, new diffraction peaks appear at scattering angles different from the Bragg positions corresponding to the space groups $Pbnm$ or $P2_1/n$. This result confirms the presence of a low-temperature magnetic ordering. The magnetic reflections can be indexed by the propagation vector $\mathbf{k} = (1/2, 0, 1/2)$; this is the same propagation vector observed for the former members of the $ANiO_3$ series (A = rare earth).

A satisfactory fit of the magnetic intensities ($R_{mag} = 15\%$), considering the smallness of the magnetic peaks, was obtained for the collinear magnetic structure previously described for $NdNiO_3$.[12] The goodness of the fit, after the refinement of the crystal and magnetic structure, is shown in Figure 2, where the indices of the magnetic reflections are indicated. A view of the magnetic structure is sketched in Figure 3. In the crystallographic unit cell, all the magnetic moments of Ni^{3+} cations are considered to lie along the b axis; the propagation vector ($1/2$, 0, $1/2$) implies that, in the neighboring cells along a and c axes, the direction of the moments is antiparallel to those of the former cell. This magnetic structure is particular in the sense that each Ni^{3+} moment is ferromagnetically coupled to three nearest neighbor Ni moments, and antiferromagnetically coupled to the three other Ni moments. This fact, also observed in the former members of the $ANiO_3$ series (A = rare earth), suggested the presence of an orbital ordering e_g^1 ($d_{z^2}^1$) and e_g^1 ($d_{x^2-y^2}^1$) of the e_g Ni^{3+} orbitals. Such an ordering has not been confirmed yet, but a recent Mössbauer study of $ANi_{0.98}Fe_{0.02}O_3$ perovskites (with A = Sm, Nd) has demonstrated for $T < T_N$ the existence of two very different magnetic hyperfine field H_i ($H_{(1)} = 450-430$ kOe and $H_{(2)} = 22-15$ kOe), in agreement with the frustrated magnetic interactions induced by the substitution Ni^{3+} (e_g^1) → Fe^{3+} (e_g^2), with such e_g orbitals ordering.[13] The refined magnetic moment magnitude converged to 1.1085 μ_B, which is close to the expected value of 1 μ_B for the low-spin t_{2g}^6 e_g^1 ($S = 1/2$) configuration.

A second possible model for the magnetic structure considers the same arrangement of Ni magnetic moments but with nonequal values for alternating Ni atoms, concomitant with the charge disproportionation effect observed at RT by Mössbauer spectroscopy and high-resolution NPD data. This second model correctly fits the low-temperature NPD data, leading to the same

(12) García-Munoz, J. L.; Rodriguez-Carvajal, J.; Lacorre, P. *Phys. Rev. B* **1994**, *50*, 978.
(13) Kim, S. J.; Demazeau, G.; Presniakov, I.; Pokholok, K.; Sobolev, A.; Baranov, A.; Pankratov, D.; Ovanesyan, N. *Phys. Rev. B*, **2002**, *66*, 14427.

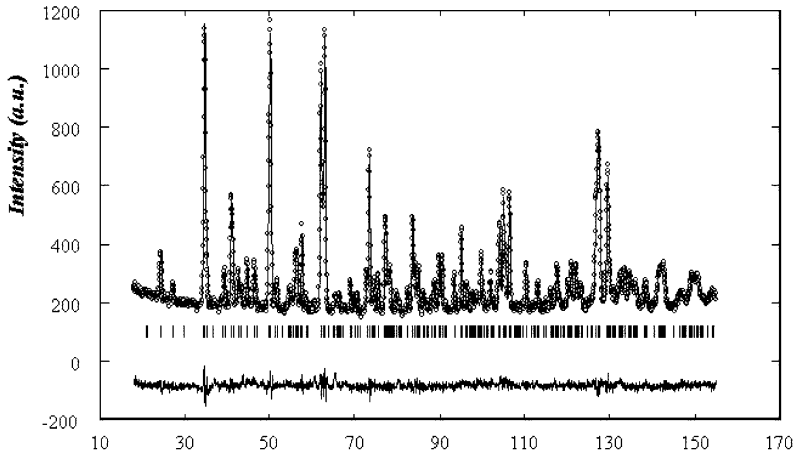

Figure 1. Rietveld refinement for neutron powder diffraction patterns of $TlNiO_3$ at room temperature. The empty circles represent the experimental data and the solid line is the calculated profile. The difference is plotted at the bottom of the figure.

Table 4. Interatomic Distances and Bond Angles for $TlNiO_3$ Refined in the $P2_1/n$ Space Group

	multiplicity	distance (Å)		angle (deg)
Tl−O1	1	2.204(3)		
Tl−O1	1	2.257(3)		
Tl−O1	1	3.157(3)		
Tl−O1	1	3.262(3)	O1−Ni1−O2	87.0(4)
Tl−O2	1	2.187(8)	O1−Ni1−O3	85.4(4)
Tl−O2	1	2.566(8)	O2−Ni1−O3	87.3(4)
Tl−O2	1	2.639(9)		
Tl−O2	1	3.429(8)		
Tl−O3	1	2.254(8)	O1−Ni1−O2	88.9(4)
Tl−O3	1	2.416(8)	O1−Ni1−O3	87.5(4)
Tl−O3	1	2.760(9)	O2−Ni1−O3	88.9(4)
Tl−O3	1	3.368(8)		
Ni1−O1	2	2.055(7)	Ni1−O1−Ni2	144.0(3)
Ni1−O2	2	1.978(5)	Ni1−O2−Ni2	145.1(2)
Ni1−O3	2	1.984(6)	Ni1−O3−Ni2	147.6(2)
<Ni1−O>		2.006	⟨Ni1−O3−Ni2⟩	145.6
Ni2−O1	2	1.919(7)		
Ni2−O2	2	1.959(6)		
Ni2−O3	2	1.926(5)		
⟨Ni2−O⟩		1.935		

discrepancy factors upon the magnetic intensities (R_{mag} = 15%). In this case, the refined magnetic moments for Ni1 and Ni2 positions converge to 1.35(17) and 0.81(17) μ_B, respectively.

The current data do not allow us to distinguish between both models for the magnetic structure (equal or unequal moments for adjacent Ni moments), although the second possibility is appealing since it is compatible with the charge disproportionation effect, which implies an accumulation of extra electrons at the Ni1 sites at the expense of inducing charge defects at the adjacent Ni2 sites. Notice that the moment values determined for the second model are very close to those obtained for $YNiO_3$ at 1.5 K,[7] for which the moment magnitudes are 1.4(1) and 0.7(1) μ_B, respectively, for Ni1 and Ni2 sites.

Magnetic Measurements. To check if ^{57}Fe was substituted to Ni, the thermal variation of χ_M^{-1} was compared to that measured for undoped $TlNiO_3$ (Figure 4). The shift of the T_N value from ≈105 K ($TlNiO_3$) to 94 K ($TlNi_{0.98}{}^{57}Fe_{0.02}O_3$) confirms the Fe → Ni substitution in the perovskite lattice and suggests a weakening of the local antiferromagnetic interactions probably due to the "frustration" of antiferromagnetic couplings through the substitution of low-spin Ni^{3+} ($t_{2g}{}^6e_g{}^1$) by high-spin Fe^{3+} ($t_{2g}{}^6e_g{}^2$) on the basis of the antiferromagnetic ordering proposed by García-Muñoz et al.[12]

Figure 5 shows the magnetization vs magnetic field plots for $TlNiO_3$ at 2, 30, and 150 K. In the magnetically ordered region, at 30 K, the M/H behavior is perfectly linear, as expected for an antiferromagnet. At 2 K there is a small deviation from linearity, with a slight hysteretic behavior and a saturation magnetization of 10^{-3} μ_B/Ni. This could correspond to a very weak ferromagnetism effect, developing at temperatures below 30 K. Of course, such a weak effect could not be detected by neutron diffraction at 2 K.

Mössbauer Investigations of $TlNi_{0.98}{}^{57}Fe_{0.02}O_3$. The spectrum of $TlNi_{0.98}{}^{57}Fe_{0.02}O_3$ at 300 K can be described as the superposition of two quadrupole doublets (Figure 6). The characteristic Mössbauer parameters are given in Table 5. The existence of two different values for both the isomer shift (δ) and the quadrupole splitting (Δ) indicates that dopant trivalent iron cations are located in two different crystallographic sites. This result is consistent with the mentioned neutron diffraction analysis, which suggests the "splitting" of the nickel positions: $Ni^{(3-\alpha)+}(1)$ and $Ni^{(3+\alpha)+}(2)$. Considering that the δ value for Fe^{n+} cations increases when the formal valence (n) decreases,[14] the subspectrum with larger δ_1 value must been related to trivalent Fe1 cations replacing nickel on $Ni^{(3-\alpha)+}O_6$ octahedra. The second quadrupole doublet with smaller δ_2 value may be related to Fe2 cations in $Ni^{(3+\alpha)+}O_6$ sites.

With use of the experimental $\delta_{1(2)}$ values and the empirical relation $\delta_i = 1.25 - 0.3n_i$ derived for high-spin iron in $Fe^{n+}O_6$ octahedra,[14] the formal valences (n_i) for Fe1 and Fe2 cations were calculated as $n_1 = 2.97$ and $n_2 = 3.40$, respectively. The difference between these values $\Delta n = 0.43$ is consistent with the difference $\Delta v = 0.53$ between the valences for Ni1 ($v_1 = 2.54$) and Ni2 ($v_2 = 3.07$) cations in $TlNiO_3$, the latter being calculated using bond-valence Brown's model,[15] which relates the bond length r_i (Table 4) and the valence (v) of the atom: $v = \sum s_i$ (s_i, valence of a bond: $s_i = \exp[(r_o - r_i)/B]$; $r_o = 1.686$, $B = 0.37$ for the $Ni^{3+}-O^{2-}$ pair. This finding provides independent quantitative evidence for a charge disproportionation phenomenon associated

(14) Menil, F. *J. Phys. Chem. Solids* **1985**, *46*, 763.
(15) Brown, I. D. *Z. Kristallogr.* **1992**, *199*, 255.

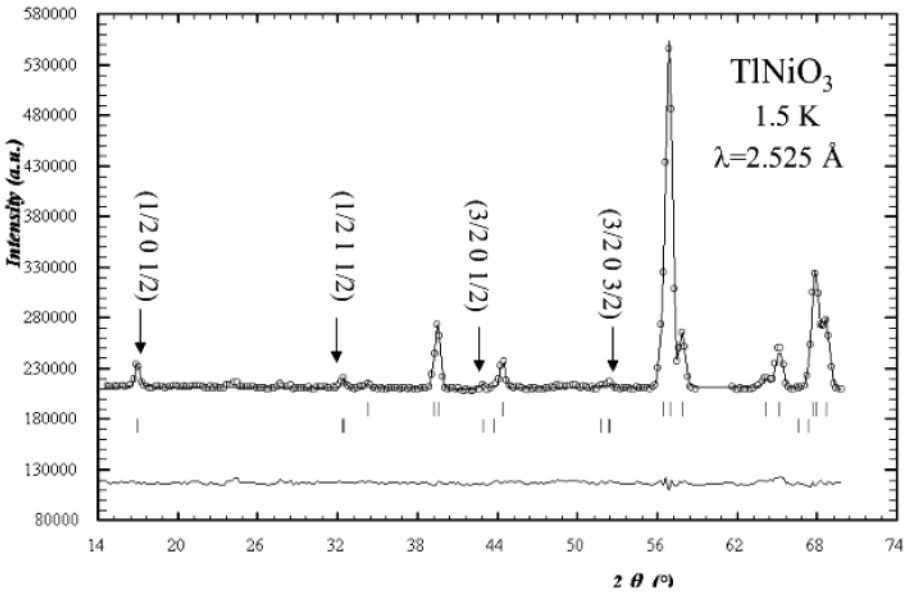

Figure 2. Rietveld plot for the low-temperature NPD data collected with a D1B diffractometer. The two series of tick marks correspond to the allowed reflections for the crystal and magnetic structure.

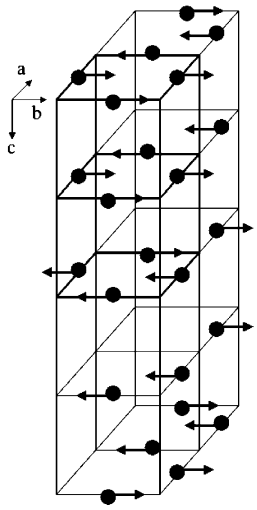

Figure 3. Schematic view of the magnetic structure of $TlNiO_3$. For the sake of clarity, in the three cells adjacent to the chemical cell (thick lines) some representative moments are only depicted. This model considers that all the magnetic moments are equivalent in magnitude, although the possibility of having alternating large and small moments in adjacent Ni positions (see text) is not discarded.

with the insulating phase of $TlNiO_3$ perovskite. However, it should be noted that δ_1 and δ_2 values clearly indicate the differing chemical environments of the two Fe1 and Fe2 sites, but do not reach the ideal values expected for a full disproportionation of Fe^{3+} into Fe^{4+} and Fe^{2+}.

The correlation of quadrupole splittings $\Delta_1 > \Delta_2$ for Fe1 and Fe2 sites is in agreement with the distortion parameters $\Delta_{d1} = 3.04 \times 10^{-4}$ and $\Delta_{d2} = 0.81 \times 10^{-4}$ of $Ni2O_6$ octahedra, concerning the deviation of Ni−O distances with respect to the average ⟨Ni−O⟩ value: $\Delta_d = (1/6)\sum_{n=1,6}[(d_n - \langle d\rangle)/\langle d\rangle]^2$, where $\langle d\rangle$ is the average bond length (Table 4). The unequal distribution of dopant Fe cations on the two sites ($A_1 > A_2$, Table 5) may be induced by the steric factors: the trivalent iron cations prefer $Ni1O_6$ sites rather than the $Ni2O_6$ ones since average $\langle Fe^{III}-O\rangle$ bonds distance (2.03 Å) in FeO_6 octahedra for ferric oxides is closer to the average bond distance ⟨Ni1−O⟩ than to that of Ni2−O bonds (Table 4).

To obtain more information concerning the behavior of $TlNiO_3$ at low temperature, a Mössbauer study was carried out at 4.2 K. Figure 7 shows the magnetic splitting due to the antiferromagnetic ordering of the Ni(Fe) sublattice. At 4.2 K, the Mössbauer spectrum can be reasonably fitted within two sets of magnetic lines whose intensity ratio corresponds to that one found in the paramagnetic region (≈2.03). The most remarkable feature of both magnetic subspectra is that the outer lines broaden while the inner lines grow in intensity at the cost of the former ones. This line shape of the Zeeman sextets indicates the presence of relaxation effects. Within the relaxation model, the broadening of the Mössbauer spectral lines is attributed to the effect of the iron spin fluctuations on a time scale of $1/\Omega_L$, where Ω_L is the Larmor precession frequency of the ^{57}Fe nucleus. Therefore, we fitted this spectrum with the sum of two magnetically split relaxation sub spectra using the model based on the stochastic relaxation theory of Blume and Tjön.[16] The magnetic hyperfine field (H), isomer shift (δ), and quadrupole perturbation (ϵ) for each Fe1 and Fe2 sites are given in Table 6, together with appropriate values for the frequency (Ω) of the spin flip process and the magnetic ordering parameter (p).

The δ_1 and δ_2 values for both Fe1 and Fe2 subspectra increase, with respect to the room-temperature values, due to the second-order Doppler effect. The H_1 and H_2 values are typical for high-spin Fe^{3+} cations, when the magnetic ordering is three-dimensional. The increased covalence of Fe^{3+}−O bonds in $Fe2O_6$ octahedra as compared to $Fe1O_6$ is reflected in lower δ_2 and in higher H_2 values. It is interesting to note that the magnitude of the relaxation frequency Ω_1 is larger than Ω_2 by 1 order of magnitude. This result is consistent with the mentioned second model for the magnetic structure of

(16) Blume, M.; Tjon, J. A. *Phys. Rev.* **1968**, *165*, 446.

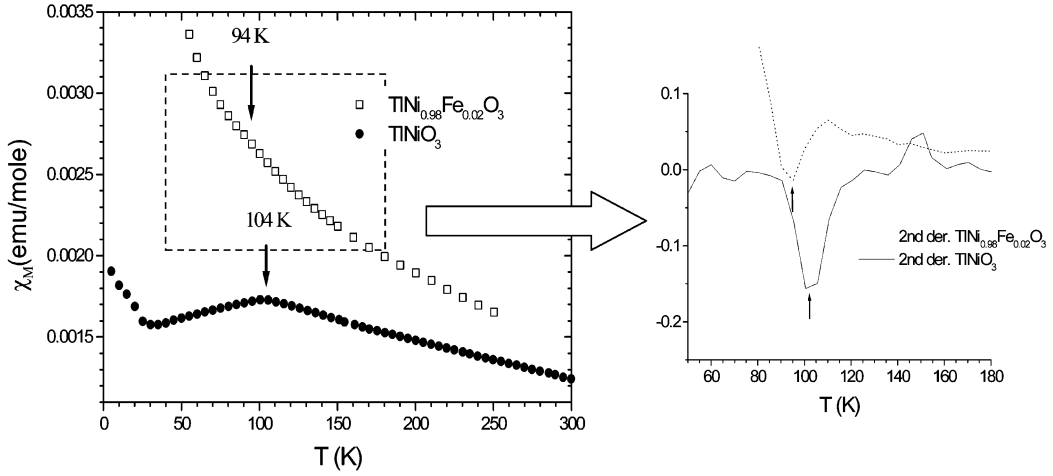

Figure 4. Temperature dependence of molar magnetic susceptibility for $TlNiO_3$ and $TlNi_{0.98}Fe_{0.02}O_3$. The T_N of $TlNi_{0.98}Fe_{0.02}O_3$ is determined from the second derivative of the magnetic susceptibility.

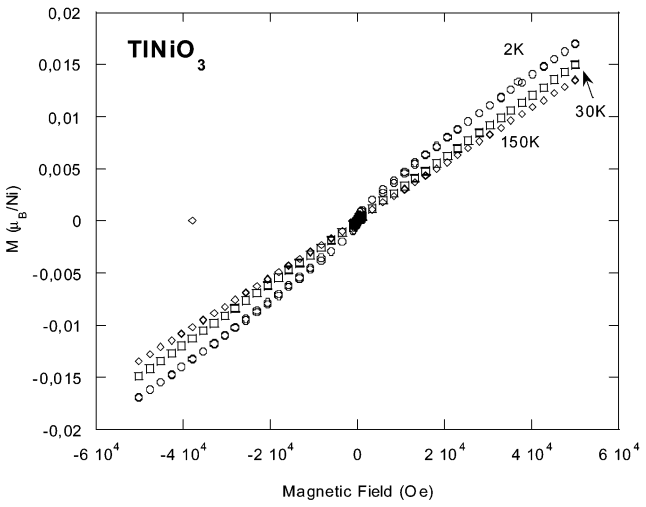

Figure 5. Magnetization vs field isotherms at $T = 2$, 30, and 150 K for $TlNiO_3$.

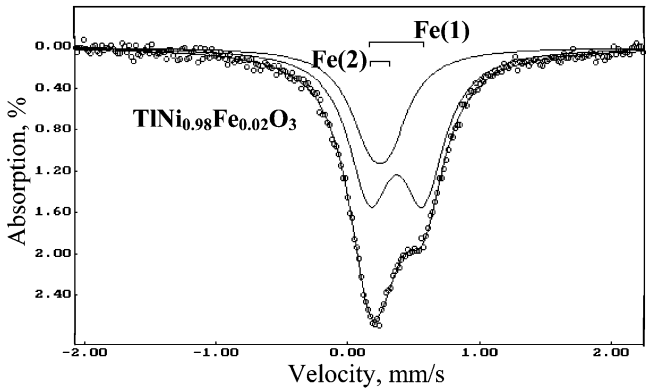

Figure 6. ^{57}Fe Mössbauer spectrum of $TlNi_{0.98}Fe_{0.02}O_3$ at 300 K.

Table 5. Mössbauer Parameters for $TlNi_{0.98}Fe_{0.02}O_3$

T (K)	Fe site	δ (mm/s)	Δ (mm/s)	Γ (mm/s)	A%
300	Fe(1)	0.36(1)	0.40(1)	0.31(1)	67(2)
	Fe(2)	0.23(1)	0.18(1)	0.30(1)	33(2)

$TlNiO_3$, which implies unequal magnetic moment values for Ni1 and Ni2 sites. In the ^{57}Fe-doped perovskite structure, $TlNi_{0.98}Fe_{0.02}O_3$, each Fe1 cation is coupled with six nearest neighboring Ni2, whereas Fe2 is coupled with six Ni1 cations. Taking into account that the Ni2 positions tend to a diamagnetic state ($\mu_{Ni2} < \mu_{Ni1}$), the Fe1−O−Ni2 superexchange interactions are expected to be very weak compared with those between the nearest neighbors Fe2−O−Ni1. As a result of the weakening of magnetic interactions, the rapid relaxation of the Fe1 spins is expected, in comparison with that observed for Fe2 cations, allowing the experimental relation to be explained: $\Omega_1 \gg \Omega_2$. Unfortunately, the poor statistics of the spectrum, even after a long accumulation time, made a more detailed analysis difficult.

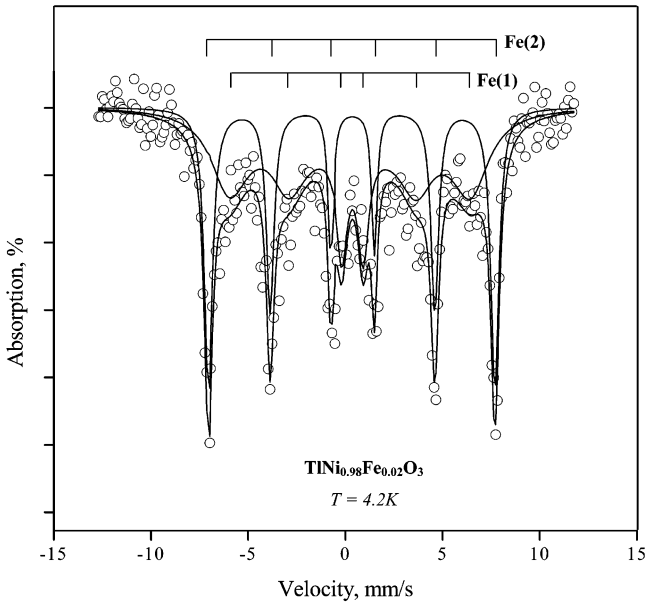

Figure 7. ^{57}Fe Mössbauer spectrum of $TlNi_{0.98}Fe_{0.02}O_3$ at 4.2 K.

Table 6. Mossbauer Parameters for $TlNi_{0.98}Fe_{0.02}O_3$ at $T = 4.2$ K

sites	δ (mm/s) (±0.02)	ϵ (mm/s) (±0.02)	H (kOe) (±3)	Γ^a (mm/s)	P	Ω (s^{-1}) ($\times 10^7$)	S (%) (±5)
Fe(1)	0.51	−0.13	405	0.30	0.75	4.50	62
Fe(2)	0.39	−0.04	461	0.30	0.98	0.12	38

[a] The corresponding values were fixed in processing the spectrum.

Conclusions

The presence of a charge disproportionation effect for Ni^{3+} cations at the $TlNiO_3$ lattice has been suggested by two independent tecniques: a neutron diffraction analysis showed that a better structural refinement is achieved in the monoclinic $P2_1/n$ space group, with two crystallographically independent Ni sites; the Mössbauer spectroscopy of a ^{57}Fe-doped sample also shows that Fe cations occupy two different crystallographic sites. The charge disproportionation of Ni^{3+} cations is a result of the improved electronic localization in $TlNiO_3$, due to the strengthening of the Tl−O bonds and concomitant weakening of the Ni−O chemical bonding. This effect is comparable to that observed in other $ANi^{3+}O_3$ perovskites in the insulating regime, below the metal−insulator transition, which has been correlated with the closing of the Ni−O−Ni angles and subsequent reduction in the overlap between Ni 3d and O 2p orbitals, resulting in the electronic localization and charge disproportionation phenomena.

Acknowledgment. The authors thanks the French Ministry of Foreign Affairs for the Pasteur Scholarship of S. J. Kim, and the Spanish Ministry of Science and Tecnology for funding the project MAT2001-0539.

CM021157O